Epithelioid and spindle cell rhabdomyosarcoma of the rib with FUS-TFCP2 fusion: A case report and literature review

DANLI YE[1*], MIN WU[1*], JIAWEN ZONG[1], WEIPENG ZENG[1], GUANGNING YAN[1], JUAN ZHOU[2] and WEI WANG[1]

[1]Department of Pathology, General Hospital of Southern Theater Command, People's Liberation Army of China, Guangzhou, Guangdong 510010, P.R. China; [2]Department of Oncology, General Hospital of Southern Theater Command, People's Liberation Army of China, Guangzhou, Guangdong 510010, P.R. China

Received September 11, 2025; Accepted December 4, 2025

DOI: 10.3892/ol.2026.15468

Abstract. Rhabdomyosarcoma (RMS) with FUS RNA binding protein-transcription factor cellular promoter 2 (FUS-TFCP2) fusion is categorized as a subtype of spindle cell/sclerosing RMS. The current study reports a case of rib RMS with FUS-TFCP2 fusion in a 29-year-old male patient who presented with a rib mass that had existed for 3 months without causing any discomfort. A computed tomography scan revealed an occupying lesion at the second rib bone with a surrounding soft-tissue mass, along with left cervical lymph node metastasis. Histologically, the tumor was composed of fascicles of spindle to epithelioid cells, some of which showed eccentric nuclei resembling rhabdomyoblasts. The stroma was collagenous/sclerotic and occasionally myxoid. Immunohistochemistry revealed positive expression for desmin, myoblast determination protein 1 and smooth muscle actin, with partial expression of anaplastic lymphoma kinase, pan-CK and myogenin. Next-generation sequencing confirmed FUS-TFCP2 fusion and showed deletions in cyclin-dependent kinase inhibitor (CDKN)2A and CDKN2B. Fluorescence *in situ* hybridization using a break-apart probe showed a translocation of TFCP2. Left cervical lymph node metastasis was confirmed. The patient succumbed to the disease 4 months after surgery. RMS with FUS-TFCP2 fusion is rare, highly aggressive and associated with a poor prognosis.

Correspondence to: Dr Wei Wang, Department of Pathology, General Hospital of Southern Theater Command, People's Liberation Army of China, 111 Liuhua Road, Guangzhou, Guangdong 510010, P.R. China
E-mail: ricewang79@126.com

*Contributed equally

Key words: rhabdomyosarcoma, epithelioid and spindle cell, FUS RNA binding protein, transcription factor cellular promoter 2, fusion, rib

Introduction

Rhabdomyosarcoma (RMS) is a non-epithelial malignant tumor that differentiates into immature skeletal muscle with rhabdomyoblastic differentiation (1). The 2020 WHO classification of tumors of soft tissue and bones has introduced new subtypes of spindle cell/sclerosing RMS (SS-RMS). SS-RMS exhibit significant clinical and genetic heterogeneity. Based on molecular characteristics, SS-RMS can be further subdivided into i) congenital/infantile spindle cell RMS, which contains gene fusions involving vestigial-like family member 2, nuclear receptor coactivator 1/2 (NCOA1/2) and serum response factor (2,3); ii) ss-RMS with myogenic differentiation 1 mutations (4); and iii) intraosseous RMS with EWS RNA binding protein 1/FUS RNA binding protein-transcription factor cellular promoter 2 (EWSR1/FUS-TFCP2) fusions (collectively referred to as FET-TFCP2 fusion RMS) or Meis homeobox 1-NCOA2 fusions (5).

RMS with TFCP2 rearrangements (TFCP2-RMS) were first described in 2018 (6). The tumor consists of spindle and epithelioid cells, predominantly occurs in the craniofacial bones and most commonly affects the mandible. TFCP2-RMS exhibits positive expression of myogenic markers, including desmin, myogenin and myoblast determination protein 1 (MyoD1), positive expression of epithelial markers, such as pan-CK and epithelial membrane antigen (EMA), and anaplastic lymphoma kinase (ALK) upregulation (5). The tumor has a predilection for the craniofacial bones, particularly the jaws of young adults, and is often associated with a rapid clinical course and poor prognosis (7).

To the best of our knowledge, to date, a total of 108 cases have been reported, mainly affecting the craniofacial bones, with only 1 case occurring in the rib (8). The present study reports an additional case of TFCP2-RMS occurring in the rib and reviews the relevant literature. The aim of the present study is to enhance the understanding of this rare subtype of RMS by summarizing its clinicopathological features, immunophenotype, molecular alterations and prognosis.

Case report

Case presentation. A 29-year-old male was admitted to the General Hospital of Southern Theater Command (Guangzhou,

China) in June 2023 with a 3-month history of an asymptomatic rib mass. A computed tomography scan demonstrated a destructive lesion arising from the second rib bone with a surrounding soft-tissue mass, measuring ~51x40 mm in diameter. The mass showed mild enhancement after contrast, along with left cervical lymphadenopathy (Fig. 1A and B). The patient underwent surgical resection of the tumor in the left second rib and a left cervical lymph node dissection.

Gross examination revealed that the tumor exhibited a destructive growth pattern, with erosion of the rib and absence of normal bone tissue. The tumor appeared solid, grayish-white and firm in consistency (Fig. 1C). Microscopically, the neoplasm exhibited a biphasic population of spindled and epithelioid tumor cells. The spindled component was arranged in intersecting fascicles with focal, ill-defined storiform architecture and displayed permeative infiltration of osseous trabeculae (Fig. 2A and B). The epithelioid cells were arranged in small clusters, nests or cords, with eosinophilic cytoplasm and rhabdoid features, vesicular nuclei and prominent nucleoli (Fig. 2C and D). The tumor cells demonstrated marked cytological atypia and frequent mitotic activity. The tumor showed marked collagenous/sclerotic and occasionally myxoid stroma. The tumor cells had metastasized to the left cervical lymph nodes (Fig. 2E). Immunohistochemical analysis revealed that the tumor cells exhibited focal positivity for CK (Fig. 2F), myogenin (Fig. 2G), ALK (Fig. 2H) and S-100 (Fig. S1A). Diffuse positivity was observed for α-smooth muscle actin (SMA), myogenic differentiation 1 (MyoD1), desmin and vimentin (Fig. S1B-E). The tumor cells were negative for SRY-box transcription factor 10 (SOX-10), cyclin-dependent kinase 4 (CDK4), mouse double minute 2 (MDM2), special AT-rich sequence binding protein 2 (SATB2), friend leukaemia virus integration 1 gene (Fli-1) and cluster of differentiation 34 (CD34) proteins (Fig. S1F-K). Additionally, the expression of trimethylated histone H3 at lysine 27 (H3K27me3), Brahma-related gene 1 (BRG-1) and integrase interactor-1 (INI-1) retained intact expression (Fig. S1L-N). The Ki-67 proliferation index was approximately 30% (Fig. S1O). Next generation sequencing (NGS) revealed TFCP-FUS gene fusion and deletion of CDKN2A and CDKN2B. Fluorescence *in situ* hybridization (FISH) using a break-apart probe showed a translocation of TFCP2 (Fig. 2I). The patient did not receive postoperative adjuvant radiotherapy/chemotherapy due to: i) TFCP2-rearranged rhabdomyosarcoma being an extremely rare, highly aggressive subtype with no recognized standard adjuvant regimen and limited response to conventional chemotherapy; and ii) rapid postoperative deterioration of the patient's general condition precluding treatment tolerance, following full family communication. The patient succumbed 4 months after surgery.

Materials and methods

Hematoxylin-eosin (H&E) staining and Immunohistochemistry (IHC). Tissue samples for conventional microscopy were processed as follows: Fixation in 10% neutral buffered formalin at 37˚C for 12 h, followed by sequential routine dehydration, clearing and paraffin embedding. Following section preparation at a thickness of 4 μm, the sections were subjected to H&E staining. Briefly, after deparaffinization in xylene and rehydration through a graded ethanol series, the sections were stained with hematoxylin at room temperature for 3-8 min, differentiated in 1% acid alcohol at room temperature for several seconds, and then blued in running tap water or a weak alkaline solution at room temperature. Subsequently, the sections were counterstained with eosin Y solution at room temperature for 1-3 min. Finally, the sections were dehydrated through an ascending alcohol series, cleared in xylene and mounted with a resinous medium. The stained sections were used for subsequent microscopic observation with an Olympus BX43 upright biological light microscope (Olympus Corporation). The formalin-fixed paraffin-embedded (FFPE) tissue sections were deparaffinized and rehydrated using xylene and graded alcohols. Following antigen retrieval, sections were blocked with 10% normal goat serum (cat. no. X090710; Agilent Technologies, Inc.) at room temperature for 30 min to reduce non-specific binding. The sections were incubated overnight at 4˚C with one of the following primary antibodies. Staining was performed with ready-to-use antibodies, including Pan-CK (cat. no. RTU-AE1/AE3-601-QH; QuanhHui International Trading Co., Ltd.), MyoD1 (cat. no. IHC630-7; GenomeMe Lab, Inc.), Ki67 (cat. no. ZM-0166; Beijing Zhongshan Jinqiao Biotechnology Co., Ltd.), SMA (cat. no. ZM-0003; Beijing Zhongshan Jinqiao Biotechnology Co., Ltd.), vimentin (cat. no. RTU-Vim-U9-QH; QUANHUI), SOX-10 (cat. no. ZA-0624; Beijing Zhongshan Jinqiao Biotechnology Co., Ltd.), CDK4 (cat. no. ZA-0614; Beijing Zhongshan Jinqiao Biotechnology Co., Ltd.), MDM2 (cat. no. ZM-0425; Beijing Zhongshan Jinqiao Biotechnology Co., Ltd.), SATB2 (cat. no. ZM-0163; Beijing Zhongshan Jinqiao Biotechnology Co., Ltd.), Fli-1 (cat. no. RTU-FLI-1-QH; QUANHUI), CD34 (cat. no. ZA-0550; Beijing Zhongshan Jinqiao Biotechnology Co., Ltd.), H3K27me3 (cat. no. RMA-0843; Fuzhou Maixin Biotech Co., Ltd.), BRG-1 (cat. no. ZA-0673; Beijing Zhongshan Jinqiao Biotechnology Co., Ltd.) and INI-1 (cat. no. ZA-0696; Beijing Zhongshan Jinqiao Biotechnology Co., Ltd.) on the Dako Link48 platform (Agilent Technologies, Inc.). External positive control tissues were provided for each slide to validate staining specificity. Subsequently, the sections were incubated with the secondary antibody using the ready-to-use Dako Real Envision Detection System (HRP-labeled polymer; cat. no. K5007; Agilent Technologies, Inc.) at room temperature for 30 min, and were stained using the Dako Real Envision kit (Agilent Technologies, Inc.). The sections were then observed using an Olympus BX43 upright biological light microscope.

Fluorescence in situ hybridization (FISH). FISH was performed on 4-μm FFPE sections with a TFCP2 (12q13) break-apart probe (Guangzhou Amoytop Medical Technology Co., Ltd.) according to the manufacturer's instructions. Briefly, the procedure was as follows: 4 μm FFPE tissue sections were baked at 65˚C for 12-16 h, deparaffinized in xylene and rehydrated through graded alcohols. Subsequently, the sections were boiled at 100˚C for 25 min, digested with pepsin for 10 min and then dehydrated to dryness via graded alcohols. Under dark conditions, 10 μl of hybridization solution containing the probe was added to the sample area, followed by cover slipping and sealing. The sections were denatured at 85˚C for 5 min and then hybridized at 37˚C for 10-18 h. After hybridization,

Figure 1. Imaging and gross pathological features of the rib tumor. (A) Non-enhanced CT: Osteolytic destruction in left second rib (red arrow) with a soft-tissue mass (51x40 mm). (B) Contrast-enhanced CT: Lymph nodes in the left supraclavicular fossa and axilla (largest: 20x12 mm, mild enhancement; red circle indicates the supraclavicular node). (C) Gross specimen: Grayish-white cut surface with firm consistency and extensive bone destruction. CT, computed tomography.

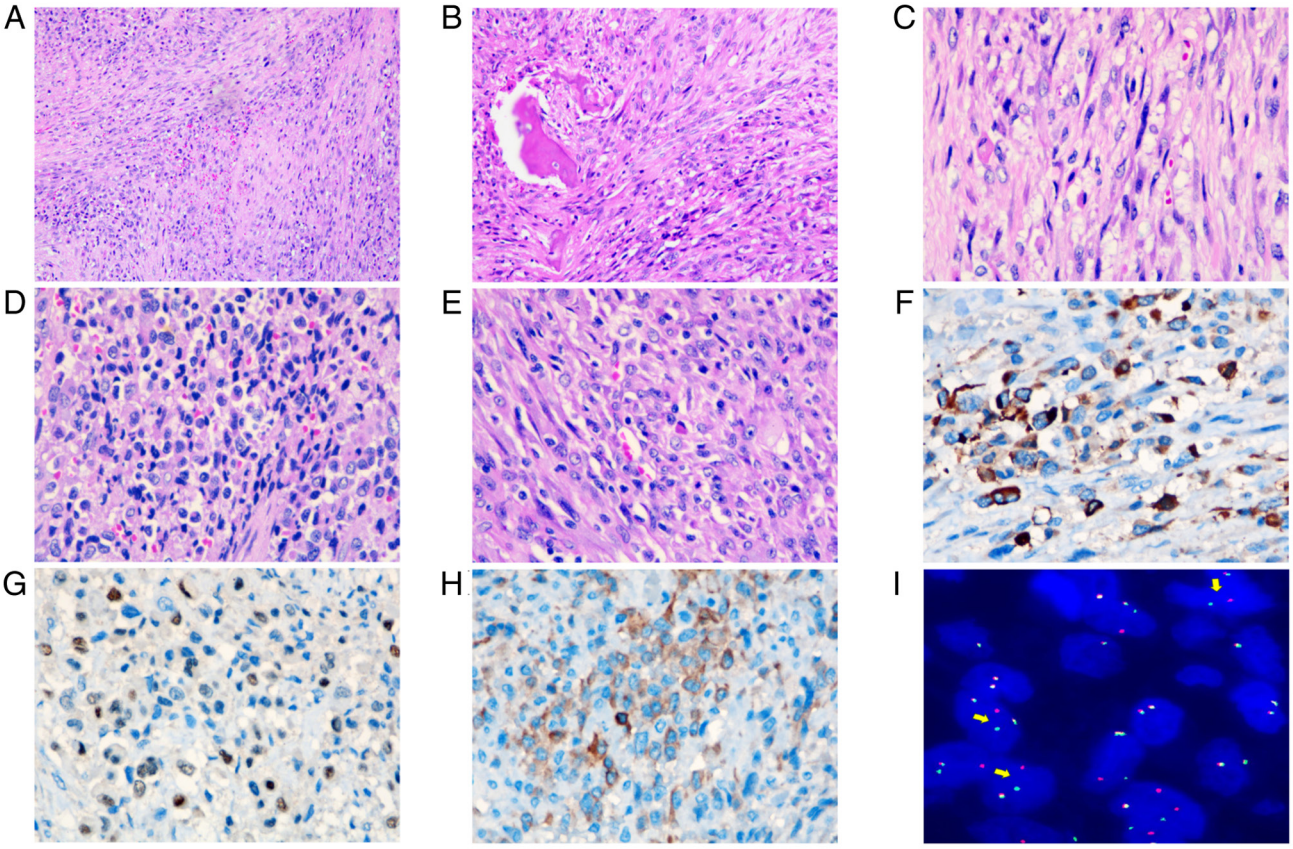

Figure 2. Histopathological and molecular features. (A) Spindle cells, arranged in fascicles infiltrating osseous trabeculae (H&E staining; x200 magnification). (B) Permeative bone invasion (H&E staining; x200 magnification). (C) Rhabdoid cells (H&E staining; x400 magnification). (D) Epithelioid cells: Eosinophilic-amphophilic cytoplasm, pleomorphic hyperchromatic nuclei (H&E staining; x400 magnification). (E) Cervical lymph node metastasis: Dense spindle cells (H&E staining; x400 magnification). (F) Pan-CK (IHC staining; x400 magnification). (G) Myogenin (IHC staining; x400 magnification). (H) Anaplastic lymphoma kinase (IHC staining; x400 magnification). (I) Fluorescence *in situ* hybridization: Transcription factor cellular promoter 2 break-apart (separation of orange/green signals). H&E, hematoxylin and eosin; IHC, immunohistochemistry.

the sealing gel was removed, and the sections were washed with 0.1% NP-40/2X SSC washing buffer at 37˚C to eliminate non-specific binding. Following graded alcohol dehydration and air-drying, DAPI counterstain was applied, and the sections were incubated in the dark for a short period before observation under an Olympus BX53 fluorescence microscope (Olympus Corporation). Normal interphase nuclei exhibited two red-green fused signals, whereas the presence of one red, one green and one fused signal was indicative of TFCP2 gene breakage.

DNA and RNA NGS analysis. NGS experiments were commissioned to Hybribio Biotech Co., Ltd., for execution. For sample processing, genomic DNA (gDNA) samples were prepared using the Haipu HP FFPE Tissue gDNA Extraction Kit (magnetic bead-based; catalog no. HP036; HaploX; Shenzhen HaploS Biotechnology Co., Ltd.). In the sample quality assessment stage, the integrity of processed samples was evaluated using an Agilent 4200 Bioanalyzer (Agilent Technologies, Inc.), while sample concentrations

were quantified via quantitative polymerase chain reaction (qPCR). Sequencing was performed on the Illumina NovaSeq 6000 platform (Illumina Inc.), employing a paired-end 150 bp read length; the corresponding sequencing kit used was the NovaSeq 6000 S4 Reagent Kit v1.5 (300 cycles; catalog no. 20046933; Illumina, Inc.). The final library was loaded at a concentration of 1.8 nM, as quantified by qPCR. Differential gene expression analysis was performed using Cuffdiff within the Cufflinks package (version 2.2.1; http://cole-trapnell-lab.github.io/cufflinks/). Genes with differential expression defined as $q<0.05$ and $|\log_2(\text{fold change})|>0.8$ were further analyzed and validated by qPCR.

Literature review

Since the first report of TFCP2-RMS in 2018, 109 cases have been reported (including the current study) (Tables I and II) (5-37). A review of the literature showed that the tumors mostly affect young adults but may also occur in elderly patients and infants. The median age of diagnosis is 33 years (range, 7-86 years). There is slight female predominance, with a female to male of 1.53:1 (66:43). The majority of cases (n=92) have an intraosseous component. A total of 66 cases (60.6%) have been located in craniofacial regions, most commonly in the mandible (n=22), while other less common sites (20.2%; n=22) include the pelvic bones, spine, ilium, pubis, femurs and ribs. The remaining 19.3% (n=21) affect the soft tissues, such as the skin (11,15,25), bladder (13,36), chest wall (6), abdominal wall (13,33), peritoneum (7), mediastinum (24) and ileum (8) (Fig. 3).

Histologically, the tumors are composed of a mixture of different cellular phenotypes, including spindle cells, epithelioid cells, round cells and rhabdomyoblasts. Among the 109 cases reported in the literature (including the present case), except for 3 cases without morphological description, the most frequent pattern described is a combined spindle and epithelioid morphology (64 cases), followed by heterogeneous mixtures of two to four cell types (18 cases). Pure phenotypes include spindle cell (14 cases), epithelioid (8 cases) and round cell (2 cases).

Immunohistochemically, TFCP2-RMS invariably exhibits dual myogenic and epithelial differentiation. The myogenic compartment shows uniform, robust expression: MyoD1 (91/91; 100%), desmin (91/95; 95.8%) and myogenin (57/91; 62.6%). Epithelial commitment is reflected in diffuse, strong staining for cytokeratin (70/86; 81.4%) and EMA (13/41; 31.7%). ALK is expressed in nearly all cases (81/90; 90.0%).

Among 109 initially enrolled cases, molecular genetic testing was successfully performed on 108 cases (1 excluded due to insufficient tissue). FUS::TFCP2 fusions were identified in 67 cases (62.0%), including 1 case of dual fusion (FUS::TFCP2 and TIMP3::ALK), while EWSR1::TFCP2 fusions were detected in 38 cases (35.2%), including 1 case of triple fusion (EWSR1 exon5::TFCP2 exon2, VAX2 exon2::ALK exon2 and VAX2 intron2::ALK exon2). FISH revealed TFCP2 rearrangements with unknown partners in 3 cases (2.8%). Among 49 cases analyzed by RNA sequencing and FISH, ALK alterations included: No alterations (19/49;38.8%), focal upregulation (16/49; 32.7%), partial deletions (12/49; 24.5%) and ALK gene fusions (2/49; 4.1%).

Treatment for TFCP2-RMS primarily involves surgery, frequently supplemented with chemotherapy and/or radiotherapy. After excluding 15 undocumented cases from the literature review, 94 patients received documented treatments: 1 underwent radiation therapy, 1 received palliative care for multiple metastases, 14 had chemotherapy, 17 underwent surgery and 61 received surgery with radiotherapy and/or chemotherapy. Among these 94 patients, 19 were treated with ALK inhibitors) (7,11-13,22,24,25,31,32,37). Due to limited treatment duration and follow-up, the prognosis was unknown for 8 of these ALK-treated patients. Of the remaining 11, a subgroup of 6 experienced temporary remission before eventual disease progression, while 5 maintained stable disease while on ALK inhibitors. Follow-up information was available for 93 patients. Among the 93 patients followed up for a mean time of 34 months (median, 15 months; range, 0-108 months), 55.9% (n=52) died of the disease within a mean time of 18 months (median, 14 months; range, 1-48 months), whereas 30.1% (n=28) remained alive with disease after a mean follow-up time of 17.6 months (median, 14.5 months; range, 1-60 months), while 14.0% (n=13) were disease-free with a mean follow-up time of 27 months (median, 21 months; range, 2-108 months).

Univariate comparisons were used to statistically evaluated clinical parameters as potential predictors of overall survival (OS) in patients, using Kaplan-Meier curves and log-rank tests (Table III). The median survival time was 21 months (Fig. S2). Among the clinical parameters of sex, age, ALK status, treatment, recurrence and tumor location, patients <30 years showed the worst prognosis. Tumor location significantly impacted survival, with bone tumors arising outside the head and neck region associated with a worse prognosis. By contrast, soft-tissue tumors demonstrated no statistically significant survival difference compared with head and neck tumors (Fig. 4A). Treatment with standard chemotherapy adversely affected OS compared with surgery alone or combined modality therapy (surgery with radiotherapy and/or chemotherapy), which was potentially attributable to more advanced clinical stages at diagnosis (Fig. 4B). Patients experiencing disease recurrence also had a significantly poorer prognosis. However, no statistically significant associations were observed for sex or ALK status levels (Table III).

Discussion

TFCP2-RMS is an extremely rare tumor, with only 108 cases having been reported to date, to the best of our knowledge (6). The present study aims to broaden our knowledge about the biological behavior, histological characteristics, treatment and prognosis of these rare tumors.

Despite diverse histological patterns, TFCP2-RMS typically displays features of mesenchymal malignant neoplasms, including infiltrative growth, marked cellular pleomorphism, high mitotic activity and necrosis. Rhabdomyoblasts are either absent or only focally present. Immunohistochemistry is required to confirm a RMS diagnosis. Notably, desmin, MyoD1 and myogenin are positively expressed in TFCP2-RMS. Additionally, CK and ALK positivity are critical for diagnosing TFCP2-RMS (6,13).

Table I. Molecular genetic features.

First author, year	Age, years	Sex	Location	Myogenin	MyoD1	Desmin	CK	ALK	EMA	Molecular	ALK gene	(Refs.)
Ishiyama *et al*, 2023	58	M	Cutaneous (scalp)	+	F+	F+	+	+	NA	F::T	Fusion	(1)
Si *et al*, 2025	39	F	Mandible	-	F+	-	D+	D+	NA	T	NA	(9)
Le Loarer *et al*, 2020	16	F	Sphenoid bone	F+	+	D+	+	+	-	F::T	50% +	(7)
	26	F	Sacrum	F+	+	+	+	+	-	F::T	50% +	
	38	F	Peritoneum	F+	+	+	+	+	F+	E::T	50% +	
	32	M	Hard palate and upper lip	-	+	D+	+	-	-	E::T	WT	
	20	M	Orbito-temporo-sphenoid	F+	+	D+	+	-	-	F::T	<5% +	
	86	M	Inguinal	F+	+	+	F+	+	-	E::T	100% +	
	18	F	Femur	+	F+	D+	+	+	-	E::T	100% +	
	17	F	Cervico-occipital junction	-	+	+	NA	+	F+	F::T	100% +	
	31	M	Occipital bone	F+	D+	D+	+	+	-	F::T	100% +	
	32	M	Mandible	F+	D+	+	+	+	-	F::T	70%	
	58	F	Mandible	F+	+	D+	+	+	-	F::T	70%	
	12	F	Mandible	+	+	D+	+	+	F+	F::T	50%	
	11	F	Maxilla	F+	+	D+	W+	W+	F+	E::T	<5% +	
	25	M	Mandible	-	+	-	+	+	-	E::T	80%	
Panferova *et al*, 2022	16	F	Mandible	F+	NA	+	W+	F+	NA	E::T	NA	(10)
Duan *et al*, 2023	54	F	Lower back, skin	S+	+	+	S+	+	+	F::T,T::A	Fusion	(11)
	28	M	Maxilla	-	+	+	+	+	NA	E::T	NA	
Chen *et al*, 2022	31	F	Maxilla	-	+	P+	P+	F+	NA	E::T	NA	(12)
	49	F	Maxilla	-	+	+	-	F+	NA	E::T	NA	
Li *et al*, 2024	6-36, mid22 (n=14)	F (n=9), M (n=5)	Head and neck region (n=9), pelvis (n=2), bladder (n=1), pubic bone (n=1), abdominal wall, humerus and pubic bone (n=1)	3/14[b] +	14/14+	14/14+	8/14+	9/14+	5/14+	F::T (n=8), E::T (n=6)	14*NA	(13)

Table I. Contiued.

First author, year	Age, years	Sex	Location	Myogenin	MyoD1	Desmin	CK	ALK	EMA	Molecular	ALK gene	(Refs.)
Carrillo-Ng *et al*, 2023	26	F	Mandible	-	+	NA	+	P+	NA	F::T	WT	(14)
	59	F	Mandible	-	+	+[a]	+	+	-	F::T	WT	
Demirkesen *et al*, 2023	35	F	Scapular-skin	W+	+	+	+	+	-	F::T	Fusion	(15)
Csizmok *et al*, 2024	31	M	Mandible	NA	NA	F+	+	F+	-	F::T	Deletion	(32)
Haug *et al*, 2023	55	F	Thoracic vertebrae	-	+	+	+	+	NA	E::T	Upregulation	(17)
Chrisinger *et al*, 2020	20	F	Pelvic	S+	+	+	NA	+	NA	F::T	NA	(18)
	20-30	F	Frontal bone	-	+	-	+	P+	NA	E::T	NA	
Li *et al*, 2023	30	F	Abdominal wall	+	+	+	+	+	-	E::T	WT	(33)
Agaram *et al*, 2019	27	M	Other bone	+	+	+	+	+	NA	F::T	NA	(5)
Koutlas *et al*, 2021	15	M	Mandible	F+	+	P+	+	-	NA	E::T	NA	(19)
Dehner *et al*, 2023	21	F	Skull	+	+	+	+	+	NA	F::T	NA	(8)
	30	F	Maxilla	+	NA	+	+	NA	NA	F::T	NA	
	60	M	Right shoulder	-	+	+	+	+	NA	E::T	NA	
	18	M	Left pubic ramus	+	+	+	+	+	NA	F::T	NA	
	43	F	Maxilla	+	+	+	+	+	NA	F::T	NA	
	31	F	Posterior iliac crest	-	+	+	-	+	NA	E::T	NA	
	41	F	Pelvic	-	+	+	NA	+	NA	E::T	NA	
	32	F	L5 vertebra	-	+	+	NA	+	NA	F::T	NA	
	26	F	Left iliac bone	+	+	+	-	+	NA	F::T	NA	
	48	F	Pelvic	NA	NA	+	NA	NA	NA	F::T	NA	
	43	M	Fourth rib	+	+	+	-	+	NA	F::T	NA	
	13	M	Maxilla	+	+	+	-	NA	NA	F::T	NA	
	27	F	Maxilla	+	+	+	+	+	NA	F::T	NA	
	44	M	Ileum	NA	NA	NA	NA	NA	NA	F::T	NA	
	70	F	Mandible	+	+	+	-	-	NA	E::T	NA	
	62	F	T7 vertebra	-	+	+	NA	+	NA	F::T	NA	

Table I. Contiued.

First author, year	Age, years	Sex	Location	Myogenin	MyoD1	Desmin	CK	ALK	EMA	Molecular	ALK gene	(Refs.)
Xu *et al*, 2021	22	M	Mandible	F+	+	F+	+	+	NA	F::T	WT	(20)
	27	F	Skull	F+	+	+	+	+	NA	E::T	NA	
	20	F	Maxilla	+	NA	F+	+	+	NA	E::T	NA	
	29	M	Skull	+	+	+	+	NA	NA	E::T	WT	
	33	F	Maxilla	+	+	F+	+	+	NA	E::T	NA	
	18	M	Skull	-	NA	-	+	+	NA	F::T	WT	
	40	F	Neck superficial soft tissue	+	NA	+	+	+	NA	F::T	Deletion	
	43	F	Mandible	R +	+	+	+	+	NA	F::T	NA	
	34	M	Mandible	NA	P+	+	-	-	NA	F::T	Deletion	
	16	M	Mandible	F+	F+	F+	+	+	NA	F::T	Deletion	
Zhu *et al*, 2019	74[c]	F	Maxilla	F+	P+	+	-	+	-	F::T	WT	(16)
Silva Cunha *et al*, 2022	17	F	Maxilla	S +	+	+	NA	NA	NA	F::T	NA	(21)
Valerio *et al*, 2023	19	F	Mandible	-	+	F+	+	D+	-	F::T	Deletion	(22)
Watson *et al*, 2018	27	F	Chest wall	+	+	+	NA	NA	NA	E::T	NA	(6)
	27	F	Pelvic	+	+	+	NA	NA	NA	F::T	NA	
	27	F	Sphenoid bone	+	+	+	NA	NA	NA	F::T	NA	
Chen *et al*, 2024	40	F	Mandible	-	+	+	+	+	NA	E::T	NA	(23)
Schöpf *et al*, 2024	17	F	Iliac bone	NA	NA	NA	NA	NA	NA	F::T	WT	(24)
	60	M	Mediastinum	NA	NA	NA	NA	NA	NA	E::T	WT	
	9	F	Mandible	NA	NA	NA	NA	NA	NA	E::T	WT	
	48	M	Maxillar	NA	NA	NA	NA	NA	NA	F::T	WT	
	35	M	Occipital/nuchal soft tissue	+	+	+	+	W+	NA	F::T	Deletion	
	49	F	Mandible	NA	NA	NA	NA	NA	NA	F::T	WT	
	25	M	Shoulder soft tissue	NA	NA	NA	NA	NA	NA	E::T	Deletion	
	14	F	Maxillar	NA	NA	NA	NA	NA	NA	F::T	Deletion	
	15	F	Temporal/sphenoid bone	NA	NA	NA	NA	NA	NA	F::T	WT	
	38	M	Maxillar	NA	NA	NA	NA	NA	NA	F::T	Deletion	

Table I. Contiued.

First author, year	Age, years	Sex	Location	Myogenin	MyoD1	Desmin	CK	ALK	EMA	Molecular	ALK gene	(Refs.)
	40	F	Occipital/nuchal soft tissue	W+	F+	F+	NA	+	NA	F::T	WT	
	58	M	Ethmoidal cells/frontal sinus	NA	NA	NA	NA	NA	NA	E::T	Deletion	
Fang *et al*, 2024	13	M	Mandible	+	+	+	F+	+	-	F::T	NA	(34)
Machado *et al*, 2025	49	F	Cutaneous (left lower back)	F+	+	+	+	+	+	F::T	WT	(25)
	55	M	Cutaneous (right flank)	NA	+	F+	+	+	NA	F::T	WT	
	67	M	Cutaneous (thoracic skin)	F+	+	F+	+	+	-	F::T	Upregulation	
	25	M	Cutaneous (shoulder/back)	+	+	+	+	+	-	E::T	Upregulation, rearrangement	
Flaitz, 2022	15	F	Mandible	R +	D+	R+	NA	+	NA	F::T	NA	(26)
Plotzke *et al*, 2024	18	M	Femur	-	+	F+	+	+	NA	E::T	Upregulation	(35)
Zhong *et al*, 2024	26	M	Mandible	-	S+	+	+	+	NA	F::T	NA	(27)
Gallagher *et al*, 2023	58	M	Maxilla	+	+	+	+	+	NA	T	NA	(28)
	22	M	Maxilla	NA	+	+	+	+	NA	T	NA	
	43	F	Zygomatic region	-	+	+	+	+	NA	NA	NA	
Tagami *et al*, 2019	70	F	Lumbar vertebra	F+	+	F+	+	+	NA	F::T	NA	(29)
Dashti *et al*, 2018	72	M	Mandible	+	+	+	+	+	NA	F::T	Upregulation	(30)
Bradova *et al*, 2024	65	M	Supraumbilical area soft tissues	Few+	D+	NA	F+	D+	+	F::T	NA	(31)
	7	F	Mandible	NA	D+	Few+	F+	D+	NA	E::T,2*V::A	NA	
	51	F	Maxilla	NA	D+	NA	W+	D+	NA	F::T	NA	
Ma *et al*, 2023	8	F	Bladder	-	+	+	-	F+	NA	E::T	Deletion	(36)
Brunac *et al*, 2020	16	F	Craniovertebral junction	+	+	+	-	+	NA	F::T	NA	(37)
Present study	29	M	Lumps in the ribs	Few+	+	+	F+	F+	+	F::T	NA	

[a]The first resection specimen was desmin-negative and the second was positive. [b]Immunohistochemistry for this marker was positive in 3 of the 14 patients. [c]This case has been reported in both citations 16 and 20. ALK, anaplastic lymphoma kinase; EMA, epithelial membrane antigen; MyoD1, myoblast determination protein 1; CK, pan-cytokeratin; F, female; M, male; -, negative; +, positive; F+, focally+; R, rare; S, scattered; w, weak; D, diffuse; P, patchy; mid, median age; E::T, EWSR1::TFCP2; F::T, FUS::TFCP2; T, TFCP2 rearrangement; E::T,2*V::A, EWSR1ex5::TFCP2ex2, VAX2ex2::ALKex2 and VAX2intron2::ALKex2; F::T,T::A, FUS exon 6::TFCP2 exon 2 and TIMP3 exon 1::ALK exon 12; NA, not applicable.

Table II. Clinicopathological features.

First author, year	Age, years	Sex	Location	Cytological	Evolution	Treatment	Outcome, time in months	(Refs.)
Ishiyama *et al*, 2023	58	M	Cutaneous (scalp)	s, ro	Local recur, met to lymph node	ST	AWD, 7	(1)
Si *et al*, 2025	39	F	Mandible	s, e	No	ST, CHT, RT	AWOD, 3	(9)
Le Loarer *et al*, 2020	16	F	Sphenoid bone	s, e	Pro, local recur and met femur bone	ST, CHT	DOD, 15	(7)
	26	F	Sacrum	e	Local pro	CHT	DOD, 4	
	38	F	Peritoneum	s, e	Pro and lymphangitic cardinomatosis	CHT	DOD, 2	
	32	M	Hard palate and upper lip	s, e	Local pro	CHT	DOD, 8	
	20	M	Orbito-temporo-sphenoid	s, e	Local pro	CHT	DOD, 6	
	86	M	Inguinal	s, e	Local recur and pro	ST	DOD, 6	
	18	F	Femur	s, e	Local pro	CHT	DOD, 8	
	17	F	Cervico-occipital junction	ro	Stable with ALK inhibitor	CHT, RT, Crizotinib, alectinib	AWD, 15	
	31	M	Occipital bone	s, e	Local recur, lung met	ST	DOD, 6	
	32	M	Mandible	s	Local recur, mandible, lung, soft tissue met	ST, CHT	AWD, 14	
	58	F	Mandible	s, e	No	ST, CHT, RT	ANED, 21	
	12	F	Mandible	s, e	No	ST, CHT, RT	ANED, 21	
	11	F	Maxilla	e	Local pro	CHT, RT	DOD, NA	
	25	M	Mandible	e	No	ST, CHT	ANED, 20	
Panferova *et al*, 2022	16	F	Mandible	s	Local recur, lymph node met	ST, CHT, RT	DOD, 11.5	(10)
Duan *et al*, 2023	54	F	Lower back, skin	s, e	Lung met	ST, Crizotinib, alectinib	AWOD, 11	(11)
	28	M	Maxilla	s, ro, e	NA	ST, RT	NA, 3	
Chen *et al*, 2022	31	F	Maxilla	s	Lymph node	ST	AWD, 5	(12)
	49	F	Maxilla	s, e	Recur	ST, RT, apatinib	AWD, 32	
Li *et al*, 2024	6-36, mid2 (n=14)	F (n=9), M (n=5)	Head and neck region (n=9), pelvis (n=2), bladder (n=1), pubic bone (n=1), abdominal wall, humerus and pubic bone (n=1)	s, e(n=14)	met or recur(n=12), no (n=1),NA(n=1)	ST, CHT (n=8);ST, CHT, RT (n=5;CHT (n=1) anti-ALK [c]	DOD(n=7), AWD(n=5), AWOD(n=1), NA(n=1), 5-37	(13)
Carrillo-Ng *et al*, 2023	26	F	Mandible	s	Recur	ST, RT	AWD, 60	(14)
	59	F	Mandible	s	Recur	ST	AWD, 22	

Table II. Continued.

First author, year	Age, years	Sex	Location	Cytological	Evolution	Treatment	Outcome, time in months	(Refs.)
Demirkesen *et al*, 2023	35	F	Scapular-skin	s, e#(R)	Local recur, met to lymph node	ST, RT	AWD, 9	(15)
Csizmok *et al*, 2024	31	M	Mandible	s, e	Local recur, met to lung met	ST, CHT, RT, alectinib	DOD, 12	(32)
Haug *et al*, 2023	55	F	Thoracic vertebrae	s, e	Recur	CHT, RT	DOD, 6	(17)
Chrisinger *et al*, 2020	20	F	Pelvic	s, e, ro, rha	Met (lung, gluteal soft tissue nodules, liver, osseous)	CHT, RT	DOD, 11	(18)
	20-30	F	Frontal bone	s, e	Recur in acetabulum, iliac bone, lung	ST, CHT, RT	DOD, 17	
Li *et al*, 2023	30	F	Abdominal wall	s, e	Recur	ST, TCM	AWD, 24	(33)
Agaram *et al*, 2019	27	M	Other bone	s	NA	NA	NA	(5)
Koutlas *et al*, 2021	15	M	Mandible	s, e	Met (lymph node, bone)	ST, CHT	AWD, 7	(19)
Dehner *et al*, 2023	21	F	Skull	s, e	Local recur	RT	AWD, 2	(8)
	30	F	Maxilla	s, e	Local recur	ST, CHT, RT	DOD, 24	
	60	M	Right shoulder	s, e	Met to lymph node	ST	NA	
	18	M	Left pubic ramus	s, e	Met (lymph nodes, bone, bilateral lung, skull)	CHT	AWD, 3	
	43	F	Maxilla	s, e, rha	Met to bone	CHT	AWD, 24	
	31	F	Posterior iliac crest	s, scl	Met to bone	Palliative care	DOD, 1	
	41	F	Pelvic	s, scl	Met to bone, lung	CHT, RT	AWD, 8	
	32	F	L5 vertebra	s, scl	Met to bone, retroperitoneum, soft tissue	ST, CHT	DOD, 15.5	
	26	F	Left iliac bone	s, e	Met (lung, bone, thyroid, adrenal, liver, soft tissue)	CHT, RT	DOD, 11	
	48	F	Pelvic	s, scl	Met to lung, bone, liver	CHT	DOD, 5	
	43	M	Fourth rib	s, e	Met to soft tissue, bone	CHT, RT	DOD, 5	
	13	M	Maxilla	s, e	NA	CHT, RT	NA	
	27	F	Maxilla	s, e	NA	NA	NA	
	44	M	Ileum	s, e, rha	NA	CHT	AWD, 1	
	70	F	Mandible	s, e	NA	NA	NA	
	62	F	T7 vertebra	s, e	No	ST, CHT	DOD, 34	
Xu *et al*, 2021	22	M	Mandible	s, e	Met to lymph node	CHT, RT	NA	(20)
	27	F	Skull	s, e	Met to bone	NA	AWD, 1	
	20	F	Maxilla	s, e	Met to bone	NA	NA	

Table II. Continued.

First author, year	Age, years	Sex	Location	Cytological	Evolution	Treatment	Outcome, time in months	(Refs.)
	29	M	Skull	s, e	Met to lung	NA	AWD, 2	
	33	F	Maxilla	s, e	NA	ST	NED, 108	
	18	M	Skull	s, e	NA	NA	NA	
	40	F	Neck superficial soft tissue	s, ro, e	NA	NA	NA	
	43	F	Mandible	s, e	NA	CHT, RT	NA	
	34	M	Mandible	s, e, rha	No	CHT, RT	AWD, 10	
	16	M	Mandible	s, e, rha	Recur, met (bone, lung, lymph node)	CHT, RT	DOD, 20	
Zhu *et al*, 2019;	74[d]	F	Maxilla	s, e	Recur, met to lymph node	NA	DOD, 21	(16)
Silva Cunha *et al*, 2022	17	F	Maxilla	s, e	Recur	ST, CHT	DOD, 9	(21)
Valerio *et al*, 2023	19	F	Mandible	s, e	Recur	ST, CHT, RT, alectinib, Lorlatinib	DOD, 11	(22)
Watson *et al*, 2018	27	F	Chest wall	e	NA	NA	DOD, 5	(6)
	27	F	Pelvic	e	NA	NA	DOD, 5	
	27	F	Sphenoid bone	e	NA	NA	DOD, 5	
Chen *et al*, 2024	40	F	Mandible	s, e	No	ST, RT	AWOD, 6	(23)
Schöpf *et al*, 2024	17	F	Iliac bone	NA	Met (bone, pleura, lung)	ST, CHT, RT, alectinib, lorlatinib	DOD, 34	(24)
	60	M	Mediastinum	s	met to lung	ST, RT, crizotinib	DOD, 20	
	9	F	Mandible	NA	Local pro, met (lung, lymph nodes)	CHT	DOD, 25	
	48	M	Maxillar	s	Met (lung, lymph nodes, bone)	ST, CHT, crizotinib	DOD, 16	
	35	M	Occipital/nuchal soft tissue	s	Recur, met (lung, lymph nodes, malignant pleural effusion)	ST, ceritinib	DOD, 42	
	49	F	Mandible	s, e, rha	Met to lymph nodes	ST, CHT, RT	DOD, 36	
	25	M	Shoulder soft tissue	e	Met (lymph nodes, lung, bone)	ST, RT	AWD, 19	
	14	F	Maxillar	NA	Local pro	CHT	DOD, 14	
	15	F	Temporal/sphenoid bone	s, e, rha	Local pro	CHT, RT	DOD, 9	
	38	M	Maxillar	s, e, rha	Local relapse, NA	ST, CHT, RT, crizotinib	DOD, 48	

Table II. Continued.

First author, year	Age, years	Sex	Location	Cytological	Evolution	Treatment	Outcome, time in months	(Refs.)
	40	F	Occipital/nuchal soft tissue	s	Local relapse, NA	ST	DOD, 42	
	58	M	Ethmoidal cells/frontal sinus	s	Local pro	CHT, crizotinib	DOD, 33	
Fang *et al*, 2024	13	M	Mandible	s	Met (vertebra and chest)	ST, CHT	DOD, 6	(34)
Machado *et al*, 2025	49	F	Cutaneous (left lower back)	s, e	No	NA	NED, 4	(25)
	55	M	Cutaneous (riht flank)	e	No	ST, RT	NED, 49	
	67	M	Cutaneous (thoracic skin)	s, e	Local recur	ST, crizotinib	NED, 50	
	25	M	Cutaneous(shoulder/back)	e, rha	Lymph node, met (lung and bone)	ST, RT	DOD, 19	
Flaitz, 2022	15	F	Mandible	s, e	NA	ST, CHT, RT	NA	(26)
Plotzke *et al*, 2024	18	M	Femur	s, e	Recur, met to bone chest	ST, CHT	DOD, 25	(35)
Zhong *et al*, 2024	26	M	Mandible	s, e	Local recur	ST	DOD, 6	(27)
Gallagher *et al*, 2023	58	M	Maxilla	s, e	NA	CHT	DOD, 3	(28)
	22	M	Maxilla	s, e	NA	NA	NA	
	43	F	Zygomatic region	s, e	NA	NA	NA	
Tagami *et al*, 2019	70	F	Lumbar vertebra	s, ro, rha	No	CHT, RT	AWD, 6	(29)
Dashti *et al*, 2018	72	M	Mandible	s, e	No	ST	AWOD, 2	(30)
Bradova *et al*, 2024	65	M	Supraumbilical area soft tissues	S	No	ST	ANED, 38	(31)
	7	F	Mandible	s, e	No	RT and CHT, crizotinib	AWD, 8	
	51	F	Maxilla	s, e	No	ST	AWD, 48	
Ma *et al*, 2023	8	F	Bladder	s	Local recur, met to lung	ST, CHT	DOD, 14	(36)
Brunac *et al*, 2020	16	F	Craniovertebral junction	ro	Recur, stable with ALK inhibitor	ST, CHT, RT, crizotinib, alectinib, lorlatinib	AWD, 19	(37)
Present study	29	M	Lumps in the ribs	s, e, rha	Pro	ST	DOD, 4	

[c]5 of the 14 patients received an ALK inhibitor, but the specific individuals were not specifically identified in the records. [d] This case has been reported in both citations 16 and 20. F, female; M, male; s, spindle; e, epithelioid; ro, round; rha, rhabdoid; scl, sclerotic; #(R), histomorphology at recurrence; met, metastasis; pro, progression; recur, recurrence; mid, median age; CHT, chemotherapy; RT, radiotherapy; ST, surgery; TCM, traditional Chinese medicine; AWD, alive with disease; AWOD, alive without disease; ANED, alive no evidence of disease; DOD, dead of disease; NED, no evidence of disease; NA, not applicable.

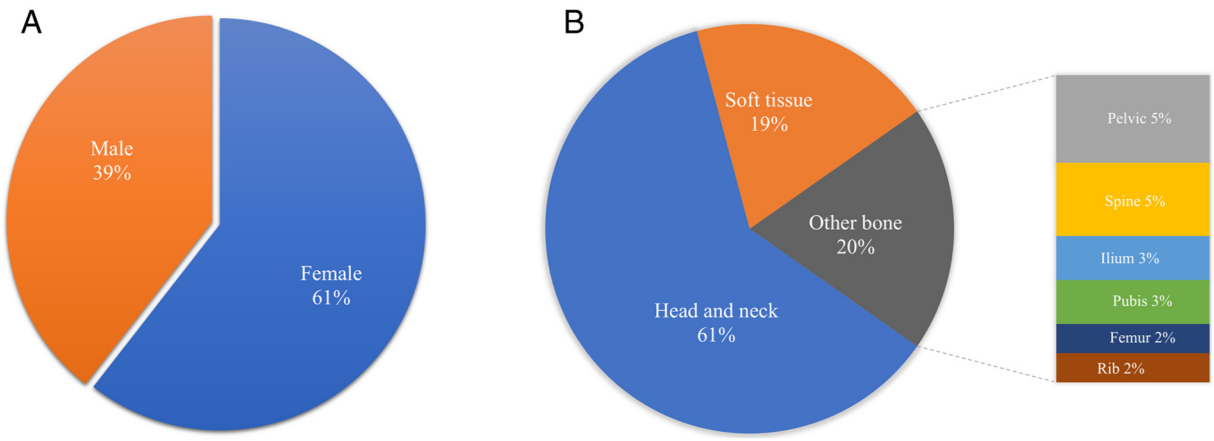

Figure 3. Distribution of cases for the TFCP2-RMS for sex and location. (A) Sex distribution of patients with TFCP2-RMS. (B) Location distribution of patients with TFCP2-RMS. TFCP2, transcription factor cellular promoter 2; RMS, rhabdomyosarcoma.

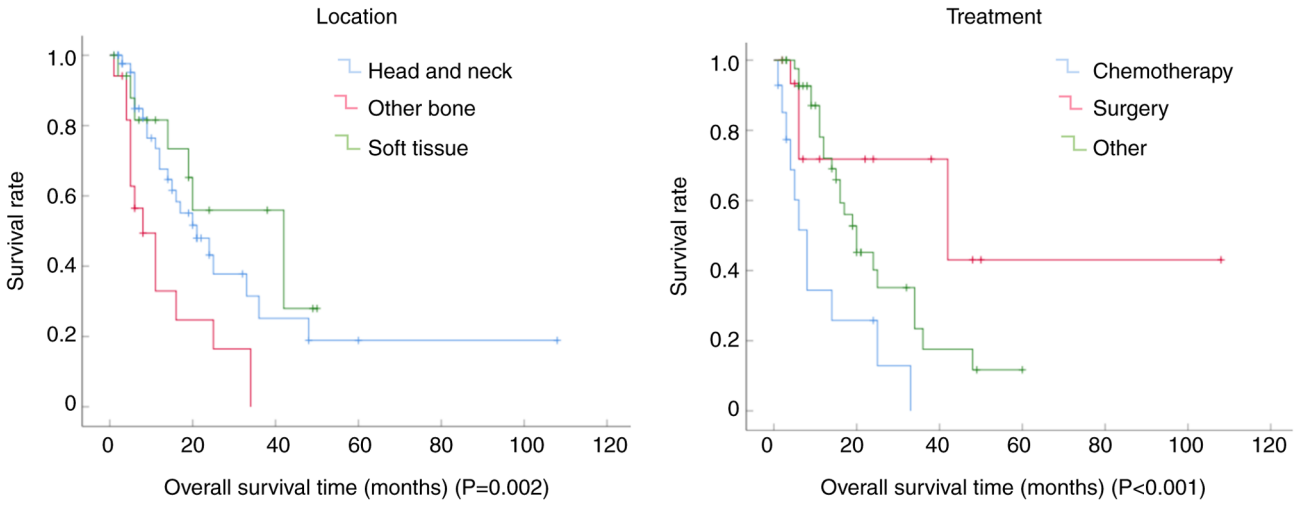

Figure 4. Overall survival analysis of patients with rhabdomyosarcoma with transcription factor cellular promoter 2 rearrangements by Kaplan-Meier univariate analysis. (A) Comparison of Kaplan-Meier curves for overall survival of patients stratified by primary tumor site (bones outside the head and neck, head and neck region, and soft tissues) (P=0.002). (B) Comparison of overall survival Kaplan-Meier curves by treatment: Standard chemotherapy, surgery alone, or surgery combined with radiotherapy and/or chemotherapy (P<0.001).

NGS-detected homozygous loss of CDKN2A/CDKN2B simultaneously disables the two key cell-cycle brakes, retinoblastoma-associated protein and tumor protein p53 (p53), in FUS-TFCP2 RMS (38). This dual disruption may explain the rapid progression of the tumor despite only moderate Ki-67 labeling, providing both a biomarker of aggressive behavior and a rationale for CDK4/6 or p53 pathway-directed therapies.

The TFCP2 gene, also known as late SV40 factor, encodes a transcription factor CP2 (also known as late SV40 factor), and is located on human chromosome 12q13.12 (12). TFCP2 plays a critical role in DNA synthesis, cell survival and anti-apoptosis by regulating cell cycle-related genes and modulating apoptosis-related genes (such as Bcl-2 family members). Aberrant TFCP2 expression or rearrangement has been implicated in diverse cancer types, including hepatocellular, pancreatic, renal, thyroid, oral, breast, cervical and colorectal cancer, where its upregulation or gene fusion drives tumor progression and correlates with a poor prognosis (39,40). For TFCP2-RMS, TFCP2 rearrangements generate fusion proteins that further augment tumor cell proliferation and aggressiveness, which may underlie the high aggressiveness and poor prognosis of this subtype.

TFCP2-RMS, a bone-predominant sarcoma, should be differentiated from metastatic sarcomatoid carcinoma, mesenchymal chondrosarcoma, osteosarcoma, dedifferentiated chondrosarcoma and epithelioid sarcoma-like hemangioendothelioma. For soft-tissue tumors, the main differential diagnoses include epithelioid hemangioendothelioma, pseudomyogenic hemangioendothelioma, pleural malignant mesothelioma, malignant peripheral nerve sheath tumor, inflammatory myofibroblastic tumor, EWSR1-POZ/BTB and AT hook containing zinc finger 1 fusion-associated spindle and round cell sarcomas, and embryonal rhabdomyosarcoma (12).

The standard treatment regimen comprises surgery combined with chemoradiotherapy. The present survival analysis demonstrated that surgical intervention alone or in conjunction with radiotherapy resulted in significantly improved overall survival compared with chemotherapy alone, which may offer critical guidance for clinical decision-making.

Table III. Overall survival of selected prognostically relevant parameters.

Concomitant variable	Standard error (95% confidence interval)	P-value
Sex	0.423 (20.170-21.830)	0.106
Age	2.929 (14.258-25.742)	0.011[a]
ALK	0.423 (20.170-21.830)	0.066
Treatment	3.704 (121.741-27.259)	<0.001[a]
Recurrence	4.166 (11.835-28.165)	0.001[a]
Location	2.929 (14.258-25.742)	0.002[a]

[a]P<0.05.

Despite a median overall survival time of 21 months reported in general, the present case presented with lymph node metastasis at diagnosis, which precluded chemotherapy, and the survival time was only 4 months. We hypothesize that tumors originating in the ribs may exhibit particularly aggressive biological behavior, a finding consistent with the observation that primary bone tumors at other sites are associated with shorter survival times than those in the head and neck. Notably, another rib case in the literature also demonstrated a limited survival time (5 months) despite receiving chemoradiotherapy without surgical resection (8).

In conclusion, TFCP2-RMS represents a rare and highly aggressive subtype of RMS; it predominantly involves the craniofacial bones in young males, with the present case being only the second reported example of rib origin. The unusual rib location and diffuse CK expression pose significant diagnostic challenges. Heightened recognition of its key clinicopathological features, predominance in young adults, epithelioid-spindled morphology, expression of rhabdomyoblastic markers and frequent ALK positivity, is therefore critical for accurate diagnosis. Molecular detection of TFCP2 translocation further confirms the diagnosis. Notably, bone tumors arising outside the head and neck, recurrence, standard chemotherapy use and age <30 years adversely impact overall survival time.

Acknowledgements

Not applicable.

Funding

This study was supported by the Natural Science Foundation of Guangdong Province of China (grant no. 2023A1515012384) and Guangdong Provincial Medical Science and Technology Research Fund (grant no. A2023190).

Availability of data and materials

The sequencing data generated in the present study are available in the NCBI SRA under accession numbers SRP650875 (BioProject) and SRR36280525 (Run). The respective URLs are: https://trace.ncbi.nlm.nih.gov/Traces/?view=study&acc=SRP65087 and https://www.ncbi.nlm.nih.gov/sra/SRR36280525. Additional data are available from the corresponding author upon request.

Authors' contributions

DLY, MW and WW conceived and designed the study. DLY and MW wrote the manuscript. JWZ, WPZ and JZ acquired MRI and CT images, and performed immunohistochemical analysis. GNY and DLY analyzed and interpreted the results. All authors have read and approved the final manuscript. DLY, MW and WW confirm the authenticity of all the raw data.

Ethics approval and consent to participate

This study involving humans was approved by the Ethics Committee of General Hospital of Southern Theater Command, People's Liberation Army of China (Guangzhou, China; approval no. NZLLKZ2025021). The study was conducted in accordance with the local legislation and institutional requirements. The participants provided their written informed consent to participate in this study.

Patient consent for publication

Written informed consent was obtained from the patient for the case information and images to be published in the present case report.

Competing interests

The authors declare that they have no competing interests.

References

1. Ishiyama T, Kato I, Ito J, Matsumura M, Saito K, Kawabata Y, Kato S, Takeyama M and Fujii S: Rhabdomyosarcoma with FUS::TFCP2 fusion in the scalp: A rare case report depicting round and spindle cell morphology. Int J Surg Pathol 31: 805-812, 2023.
2. Alaggio R, Zhang L, Sung YS, Huang SC, Chen CL, Bisogno G, Zin A, Agaram NP, LaQuaglia MP, Wexler LH and Antonescu CR: A molecular study of pediatric spindle and sclerosing rhabdomyosarcoma: Identification of novel and recurrent VGLL2-related fusions in infantile cases. Am J Surg Pathol 40: 224-235, 2016.
3. Karanian M, Pissaloux D, Gomez-Brouchet A, Chevenet C, Le Loarer F, Fernandez C, Minard V, Corradini N, Castex MP, Duc-Gallet A, *et al*: SRF-FOXO1 and SRF-NCOA1 fusion genes delineate a distinctive subset of well-differentiated rhabdomyosarcoma. Am J Surg Pathol 44: 607-616, 2020.
4. Agaram NP, LaQuaglia MP, Alaggio R, Zhang L, Fujisawa Y, Ladanyi M, Wexler LH and Antonescu CR: MYOD1-mutant spindle cell and sclerosing rhabdomyosarcoma: An aggressive subtype irrespective of age. A reappraisal for molecular classification and risk stratification. Mod Pathol 32: 27-36, 2019.
5. Agaram NP, Zhang L, Sung YS, Cavalcanti MS, Torrence D, Wexler L, Francis G, Sommerville S, Swanson D, Dickson BC, *et al*: Expanding the spectrum of intraosseous rhabdomyosarcoma: Correlation between 2 distinct gene fusions and phenotype. Am J Surg Pathol 43: 695-702, 2019.
6. Watson S, Perrin V, Guillemot D, Reynaud S, Coindre JM, Karanian M, Guinebretiere JM, Freneaux P, Le Loarer F, Bouvet M, *et al*: Transcriptomic definition of molecular subgroups of small round cell sarcomas. J Pathol 245: 29-40, 2018.
7. Le Loarer F, Cleven AHG, Bouvier C, Castex MP, Romagosa C, Moreau A, Salas S, Bonhomme B, Gomez-Brouchet A, Laurent C, *et al*: A subset of epithelioid and spindle cell rhabdomyosarcomas is associated with TFCP2 fusions and common ALK upregulation. Mod Pathol 33: 404-419, 2020.

8. Dehner CA, Broski SM, Meis JM, Murugan P, Chrisinger JSA, Sosa C, Petersen M, Halling KC, Gupta S and Folpe AL: Fusion-driven spindle cell rhabdomyosarcomas of bone and soft tissue: A clinicopathologic and molecular genetic study of 25 cases. Mod Pathol 36: 100271, 2023.
9. Si C, Wang Y and Zhu J: A rare case report of intraosseous spindle and epithelioid rhabdomyosarcoma with TFCP2 rearrangement: A pathological diagnostic conundrum and literature review. Int J Surg Pathol 33: 125-130, 2025.
10. Panferova A, Sinichenkova KY, Abu Jabal M, Usman N, Sharlai A, Roshchin V, Konovalov D and Druy A: EWSR1-TFCP2 in an adolescent represents an extremely rare and aggressive form of intraosseous spindle cell rhabdomyosarcomas. Cold Spring Harb Mol Case Stud 8: a006209, 2022.
11. Duan FL, Yang H, Gong X, Zuo Z, Qin S, Ji J, Zhou C, Dai J, Guo P and Liu Y: Clinicopathological features of rhabdomyosarcoma with novel FET::TFCP2 and TIMP3::ALK fusion: Report of two cases and literature review. Histopathology 82: 478-484, 2023.
12. Chen XY, Chen G, Zhu Q, Zhu WF, He C and Huang RF: Clinicopathological features of rhabdomyosarcoma with TFCP2 fusions. Zhonghua Bing Li Xue Za Zhi 51: 545-547, 2022 (In Chinese).
13. Li HL, Mo CH, Xie L, Wu YX, Zeng M and Mao RJ: Clinicopathological study of epithelioid and spindle cell rhabdomysarcoma with EWSR1/FUS-TFCP2 fusion. Zhonghua Bing Li Xue Za Zhi 53: 58-63, 2024 (In Chinese).
14. Carrillo-Ng H, Liang Y, Chang S, Afkhami M, Gernon T, Bell D and Arias-Stella JA: Complete mimicry: Rhabdomyosarcoma with FUS::TFCP2 fusion masquerading as carcinoma-diagnostic challenge and report of two cases. Genes Chromosomes Cancer 62: 430-436, 2023.
15. Demirkesen C, Danyeli AE, Yildiz P, Ertekin SS, Yilmaz B, Karahan SI and Bahrami A: Cutaneous rhabdomyosarcoma with FUS::TFCP2 fusion: A case report emphasizing early detection. J Cutan Pathol 50: 1059-1064, 2023.
16. Zhu G, Benayed R, Ho C, Mullaney K, Sukhadia P, Rios K, Berry R, Rubin BP, Nafa K, Wang L, *et al*: Diagnosis of known sarcoma fusions and novel fusion partners by targeted RNA sequencing with identification of a recurrent ACTB-FOSB fusion in pseudomyogenic hemangioendothelioma. Mod Pathol 32: 609-620, 2019.
17. Haug L, Doll J, Appenzeller S, Kunzmann V, Rosenwald A, Maurus K and Gerhard-Hartmann E: Epithelioid and spindle cell rhabdomyosarcoma with EWSR1::TFCP2 fusion mimicking metastatic lung cancer: A case report and literature review. Pathol Res Pract 249: 154779, 2023.
18. Chrisinger JSA, Wehrli B, Dickson BC, Fasih S, Hirbe AC, Shultz DB, Zadeh G, Gupta AA and Demicco EG: Epithelioid and spindle cell rhabdomyosarcoma with FUS-TFCP2 or EWSR1-TFCP2 fusion: Report of two cases. Virchows Arch 477: 725-732, 2020.
19. Koutlas IG, Olson DR and Rawwas J: FET(EWSR1)-TFCP2 Rhabdomyosarcoma: An additional example of this aggressive variant with predilection for the gnathic bones. Head Neck Pathol 15: 374-380, 2021.
20. Xu B, Suurmeijer AJH, Agaram NP, Zhang L and Antonescu CR: Head and neck rhabdomyosarcoma with TFCP2 fusions and ALK overexpression: A clinicopathological and molecular analysis of 11 cases. Histopathology 79: 347-357, 2021.
21. Silva Cunha JL, Cavalcante IL, da Silva Barros CC, Alves PM, Nonaka CFW, Albuquerque AFM, de Almeida OP, de Andrade BAB and Cavalcante RB: Intraosseous rhabdomyosarcoma of the maxilla with TFCP2 fusion: A rare aggressive subtype with predilection for the gnathic bones. Oral Oncol 130: 105876, 2022.
22. Valerio E, Furtado Costa JL, Perez Fraile NM, Credidio CH, Taveira Garcia MR, Neto CS and Costa FD: Intraosseous spindle Cell/Epithelioid rhabdomyosarcoma with TFCP2 rearrangement: A recent recognized subtype with partial response to alectinib. Int J Surg Pathol 31: 861-865, 2023.
23. Chen F, Wang J, Sun Y and Zhang J: Mandibular rhabdomyosarcoma with TFCP2 rearrangement and osteogenic differentiation: A case misdiagnosed as fibrous dysplasia or low-grade central osteosarcoma. Oral Surg Oral Med Oral Pathol Oral Radiol 137: e143-e149, 2024.
24. Schöpf J, Uhrig S, Heilig CE, Lee KS, Walther T, Carazzato A, Dobberkau AM, Weichenhan D, Plass C, Hartmann M, *et al*: Multi-omic and functional analysis for classification and treatment of sarcomas with FUS-TFCP2 or EWSR1-TFCP2 fusions. Nat Commun 15: 51, 2024.
25. Machado I, Wardelmann E, Zhao M, Song J, Wang Y, Braun SA, Catasus L, Ferre M, Leoveanu I, Westhoff J, *et al*: Primary cutaneous rhabdomyosarcoma with EWSR1/FUS::TFCP2 fusion: Four new cases with distinctive morphology, immunophenotypic, and genetic profile. Virchows Arch 486: 1187-1198, 2025.
26. Flaitz C, Hicks J: Primary Intraosseous Rhabdomyosarcoma: Rare Subtype Involving Mandible with Unique Translocation. Oral Surgery Oral Med Oral Pathol Oral Radiol 133: 157, 2022.
27. Zhong P, Wei S, Xiao H and Zeng Y: Rhabdomyosarcoma with *FUS::TFCP2* fusion in the mandible: A rare aggressive subtype, but can be misdiagnosed as ossifying fibroma. Int J Surg Pathol 32: 758-766, 2024.
28. Gallagher KPD, Roza A, Tager E, Mariz B, Soares CD, Rocha AC, Abrahao AC, Romanach MJ, Carlos R, Hunter KD, *et al*: Rhabdomyosarcoma with TFCP2 rearrangement or typical Co-expression of AE1/AE3 and ALK: Report of three new cases in the head and neck region and literature review. Head Neck Pathol 17: 546-561, 2023.
29. Tagami Y, Sugita S, Kubo T, Iesato N, Emori M, Takada K, Tsujiwaki M, Segawa K, Sugawara T, Kikuchi T and Hasegawa T: Spindle cell rhabdomyosarcoma in a lumbar vertebra with FUS-TFCP2 fusion. Pathol Res Pract 215: 152399, 2019.
30. Dashti NK, Wehrs RN, Thomas BC, Nair A, Davila J, Buckner JC, Martinez AP, Sukov WR, Halling KC, Howe BM and Folpe AL: Spindle cell rhabdomyosarcoma of bone with FUS-TFCP2 fusion: Confirmation of a very recently described rhabdomyosarcoma subtype. Histopathology 73: 514-520, 2018.
31. Bradova M, Mosaieby E, Michal M, Vanecek T, Ing SK, Grossmann P, Koshyk O, Kinkor Z, Laciok S, Nemcova A, *et al*: Spindle cell rhabdomyosarcomas: With TFCP2 rearrangements, and novel EWSR1::ZBTB41 and PLOD2::RBM6 gene fusions. A study of five cases and review of the literature. Histopathology 84: 776-793, 2024.
32. Csizmok V, Grisdale CJ, Williamson LM, Lim HJ, Lee L, Renouf DJ, Jones SJM, Marra MA, Laskin J and Smrke A: Diagnostic and therapeutic implications of a FUS::TFCP2 fusion and ALK activation in a metastatic rhabdomyosarcoma. Genes Chromosomes Cancer 63: e23259, 2024.
33. Li Y, Li D, Wang J and Tang J: Epithelioid and spindle rhabdomyosarcoma with TFCP2 rearrangement in abdominal wall: A distinctive entity with poor prognosis. Diagn Pathol 18: 41, 2023.
34. Fang Z, Duan C, Wang S, Fu L, Yang P, Yu T, Deel MD, Lau LMS, Ma X, Ni X and Su Y: Pediatric spindle cell/sclerosing rhabdomyosarcoma with FUS-TFCP2 fusion: A case report and literature review. Transl Pediatr 13: 178-191, 2024.
35. Plotzke JM, Rabah R, Robinson DR, Edmonds A, Bloom DA, Mody R and Heider A: Primary intraosseous spindle cell rhabdomyosarcoma: A case report in an unusual location. Pediatr Dev Pathol 27: 597-602, 2024.
36. Ma Y, Feng J, Ding D, Zhao J and Tian F: TFCP2-rearranged epithelioid and spindle cell rhabdomyosarcoma in the bladder: A rare case in an 8-year-old female child. Pediatr Blood Cancer 70: e29935, 2023.
37. Brunac AC, Laprie A, Castex MP, Laurent C, Le Loarer F, Karanian M, Le Guellec S, Guillemot D, Pierron G and Gomez-Brouchet A: The combination of radiotherapy and ALK inhibitors is effective in the treatment of intraosseous rhabdomyosarcoma with FUS-TFCP2 fusion transcript. Pediatr Blood Cancer 67: e28185, 2020.
38. Ginn MP, Denu RA, Ingram DR, Wani KM, Lazar AJ, Harrison DJ, Nakazawa MS, Conley AP, Patel S and Livingston JA: TFCP2 Fusion-Positive Rhabdomyosarcomas: A Report of 10 cases and a review of the literature. Cancers (Basel) 17: 1441, 2025.
39. Kotarba G, Krzywinska E, Grabowska AI, Taracha A and Wilanowski T: TFCP2/TFCP2L1/UBP1 transcription factors in cancer. Cancer Lett 420: 72-79, 2018.
40. Hsu WH, LaBella KA, Lin Y, Xu P, Lee R, Hsieh CE, Yang L, Zhou A, Blecher JM, Wu CJ, *et al*: Oncogenic KRAS drives lipofibrogenesis to promote angiogenesis and colon cancer progression. Cancer Discov 13: 2652-2673, 2023.

Copyright © 2026 Ye et al. This work is licensed under a Creative Commons Attribution-NonCommercial-NoDerivatives 4.0 International (CC BY-NC-ND 4.0) License.